This is an accepted manuscript entitled “Switching of Radiation Force on Optically Trapped Microparticles through Photochromic Reactions of Pyranoquinazoline Derivatives”, published in *J. Phys. Chem. C*, 122 (**2018**), 22033-22040..

To see the published version, click a link below:

https://pubs.acs.org/doi/abs/10.1021/acs.jpcc.8b03420

Switching of Radiation Force on Optically Trapped Microparticles through Photochromic Reactions of Pyranoquinazoline Derivatives

Kenji Setoura[†], Ahsan M. Memon[†], Syoji Ito[†], Yuki Inagaki[‡], Katsuya Mutoh[‡], Jiro Abe[‡], and Hiroshi Miyasaka[†*].*

[†] Division of Frontier Materials Science and Center for Promotion of Advanced Interdisciplinary Research, Graduate School of Engineering Science, Osaka University, Toyonaka, Osaka 560-8531, Japan

[‡] Department of Chemistry, School of Science and Engineering, Aoyama Gakuin University, 5-10-1 Fuchinobe, Chuo-ku, Sagamihara, Kanagawa 252-5258, Japan

ABSTRACT. Photo-control of mechanical motions of small objects has attracted much attention to develop mesoscopic remote actuators. For this purpose, photo-induced morphological changes of molecules, molecular aggregates, and crystals have been extensively studied in the field of chemistry and materials science. Here, we propose direct use of momenta of light (*i.e.* radiation force) to control the motion of small objects, through photochromic reactions of pyranoquinazoline (PQ) derivatives. PQ is colorless in visible wavelength region while it is in closed form, and undergoes photochemical ring-opening reactions to form colored isomers upon UV light irradiation; the open-ring isomers return to the colorless closed isomers mainly through the thermal back reaction. In the experiment, individual polymer microparticles with diameters of 7 μm incorporating PQ were trapped by optical tweezers. When the trapped microparticle was irradiated with UV light, the microparticle was pushed along the axis of light propagation about a few micrometers by absorption force arising from PQ in colored form. In addition, we found that dynamics of trapped microparticles was regulated by the thermal back reaction of PQ. The present results demonstrate that diversity of photochromic reactions can be transcribed into mesoscopic motions through the momentum exchange between light and molecules.

Introduction Controlled motions of mesoscopic objects have been attracting much attention in the field of nanoscience and nanotechnology from various viewpoints relating to mesoscopic actuators. Photo-irradiation is one of most promising external stimuli to control tiny objects, because of its non-contact nature and high spatial resolution.[1] Along this line, photo-responsive materials that can change their shape and size under the illumination have been so far developed in chemistry and materials science.[2–4] Photochromic compounds such as diarylethene derivatives are one of promising materials to achieve meso/macroscopic motions (*e.g.* 1 to 100 μm) through the photoisomerization reaction of individual molecules leading to the geometrical change of assemblies in meso/macroscopic scales.[5]

Contrary to this bottom-up and hierarchical approach from the molecular reaction, optical tweezers[6–8] on the basis of the optical force could be regarded as a top-down method to control mesoscopic motions of small particles with diameters of 10 nm to 10 μm. In principle, optical forces (F_{photo}) acting on the trapped objects can be divided into three terms[7,9]; gradient force (F_{grad}), scattering force (F_{sca}), and absorption force (F_{abs}). In most of the studies so far accumulated for optical tweezers, targets of trapping are under the irradiation with near infrared lasers for which the targets have no optical absorption bands.[1,8,9] In these cases, F_{grad} directs the particle into the focal spot of a laser beam and keeps it under the trapping, while F_{sca} slightly pushes the particle along the axis of light propagation.[7] Accordingly, for more sophisticated manipulation, spatial shaping of F_{grad} has been intensively investigated such as optical vortices[10,11], topological lightwaves[12], and near-field of localized surface plasmon.[13,14]

It is worth noting that F_{grad} is based on the momentum exchange between light and matter and it is essentially weak compared to the absorption force where the momenta of photons can be

resonantly transferred to the target object by the absorption of the light.[15,16] Accordingly, the F_{abs} is large enough to induce the translational motion along the optical axis as already demonstrated for quantum dots whose absorption band is resonant to the incident light.[16] In other words, versatile motions of small targets are expected by the switching of F_{abs} through the switching of the color of the object by organic photochromic molecules inside in the target. In the photochromic reaction, the initial isomer without absorption at the trapping wavelength turns to the colored one by the first switching light and the reverse process to the colored isomer is induced by another light at the wavelength different from the first one or the thermal back reaction.[5,17,18] Accordingly, reversible switching of F_{abs} through the photochromic reactions may lead to fast pushing and pulling of the objects leading to the translational motion in the mesoscopic scale. Moreover, the trapped objects could undergo the translational motion in the case where the thermal back reaction. That is, the position of the small object under the trapping could be modulated by other light for the switching the color by the photochromic reaction of small number of molecules through the resonant momentum exchange between light and molecules.

In the present work, we employed a pyranoquinazoline derivative (PQ) that instantaneously undergoes the photochemical reaction upon UV light irradiation, resulting in the formation of an isomer with the absorption bands in the whole visible wavelength region. This colored isomer returns to the colorless one by thermal back reaction with the time constant < 1 s.[19] Accordingly, we can switch the F_{abs} acting on the microparticle trapped by the laser beam whose output wavelength is resonant to the visible absorption of the colored isomer. In the actual system, PQ was put into polymer microparticles (PMPs) with diameters of *ca.* 7 μm. UV irradiation of the PMP with PQ inside under the laser trapping led to the OFF-ON switching of F_{abs}, leading to the spatial displacements (pushing) of the PMP by a few μm along the axis of light propagation. After

the UV light was turned off, the PMP returned slowly to its original trapped position, showing that the decolorization process of the thermal back reaction of PQ regulates the returning process. The present results demonstrated that various kinds of mesoscopic motions can be realized with diversity of the photochromic reactions, through the light-matter interaction on the momentum.

Results and Discussion

Photochromic reaction of pyranoquinazoline derivatives. Fig. 1a shows the molecular structure and photochromic reactions of PQ.[19] Closed-form (CF) isomer of PQ undergoes the reaction leading to the *transoid-cis* (TC) isomer upon UV irradiation. The TC isomer returns to the CF isomer through mainly by a thermal back reaction. Photoexcitation of the TC isomer leads to formation of third isomers, *transoid-trans* (TT) form, with a very small reaction yield.[19] In the present study, however, it was not necessary to take this species into account owing to the negligible production yield.

Fig. 1b shows UV-Vis absorption spectra of PQ in the CF- and the TC isomers in toluene solution at 298 K. CF isomer has an absorption band around 360 nm and is colorless in visible wavelength region, while TC isomer exhibits a broad absorption band with a maximum at 570 nm in the visible region. Polymer microparticles (PMPs) incorporating PQ were used as specimens for the laser trapping (details are shown in the methods section). So as to induce the photochromic reaction of PQ accompanying rather large changes of the molecular structure,[20] soft polymer matrices (polyacrylic ester resins) were used. Photochromic reactions of PQ in the PMP were confirmed by UV-visible absorption spectra (See Supporting Information (S.I.) S1 and Figure S1).

The absorption tail of TC isomer was slightly extended (*ca.* 50 nm) to longer wavelength region in the PMP compared with that in toluene, probably due to the difference of environments around PQ.

Optical trapping at 690 nm: F_{abs} in non-resonance. Optical trapping of the PMPs was executed under an inverted optical microscope. Mechanical motions of the trapped PMP were detected by the transmission imaging with an oil immersion objective (NA = 1.30). Trapping lasers at 532 and 690 nm were focused to diffraction-limited spots. For the photochromic reactions of PQ, the UV laser at 355 nm was coaxially introduced into the optical path of the trapping laser beam. To illuminate the trapped PMP uniformly, a spot diameter of the UV laser was expanded to 15 μm at the focal plane. All lasers were linearly polarized. A series of the trapping experiment was performed in the following manner. First, the PMP incorporating PQ was trapped by the visible laser beam. At this moment, the PMP was colorless at the trapping wavelength. Then, the PMP is irradiated with the UV light for 2 s after the video recording started. After turning off the UV light, the video recording was continued until 15 s to track the thermal back reaction of PQ. The intensity of the 690-nm laser was 500 μW at the sample position.

Fig. 2a-d shows temporal evolution of the images of the trapped PMP with PQ inside. These images were obtained by using the illumination light in the wavelength range of 488-633 nm. Accordingly, the transmission image before the UV irradiation (t = 0 s) is almost transparent. Fig. 2b shows the transmission image of the PMP at 0.06 s after the start of UV exposure with the excitation intensity of 400 mW cm^{-2}, indicating the decrease of the transmittance due to the formation of the TC isomer through the ring-opening reaction of the CF isomer. The transmission image of the PMP 0.2 s after shutting off the UV exposure in Fig. 2c shows the increase in the

transmission compared to that in Fig .2b. The color gradually faded away with an increase in the time after the termination of the UV exposure. This is due to the thermal back reaction from TC to CF isomers. After ca. 10 s following the termination of the UV irradiation, the color of the PMP recovered to the original transparent state.

In order to detect the spatial displacements of the PMP induced by F_{abs} along the Z-axis, we employed height dependence of diameters of scattered rings of the PMP.[21–23] The diameter of the scattering ring of the PMP fixed on the glass coverslip was measured at various heights by using a 3D piezo scanning stage. The relation between the diameter of scattering ring and the absolute Z-position of the PMP in the above measurements provides the calibration curve for the analysis of the Z-position under the trapping. For the detection of circular objects and the evaluation of its diameters and weight centers in all optical micrographs, we employed the hough transform method, which is available in Matlab image processing toolbox as a predefined function. The changes in diameter of the scattering ring were linear in the range of Z-position of 0 to 2 μm with an accuracy of *ca.* 100 nm. Note that the calibration coefficient of the Z-position was slightly diameter-dependent, and this dependence was taken into consideration.

Fig. 2e shows a time course of the Z-displacements of the trapped PMP. The Z-displacement starts to increase at 2 s where the UV exposure started, followed by the gradual increase with an increase in the UV exposure time. The maximum value of the displacement is *ca.* 100 nm at 4 s. After the UV laser was turned off at 4 s, the Z-displacement slowly decreases and finally came back to the original position at around 7 or 8 s. These dynamics of the displacement along the Z-position will be discussed in detail in the latter section.

To directly verify the contribution of the colorization reaction inducing F_{abs}, we performed a control experiment with no photochromic molecules. In this case, no Z-displacement was detected under UV irradiation for the bare PMP under optical trapping (See Figure S2 in S.I.). In addition, we confirmed that the colorization of the PMP incorporating PQ never affect accuracy of evaluation of Z-displacements (See Figure S3 in S.I.). From these results, we concluded that the Z-displacements observed in Fig. 2e can be ascribable to F_{abs} by the change of the color of PQ at the trapping wavelength of 690 nm.

Trapping wavelength dependence: resonant and non-resonant. To more quantitatively elucidate the contribution of F_{abs} on the trapped PMP, we employed a CW laser at 532 nm for comparison. The strong resonance absorption of the TC isomer locates at 532 nm as was shown in Fig.1, while the absorption intensity is much weaker at 690nm. Because the gradient and scattering forces and diffraction-limited spot size are also wavelength dependent, we first obtained the information on these factors by measuring the positional fluctuations of the PMP without PQ in both wavelength conditions. The fluctuation was observed to be ca. 700 nm (in fwhm in horizontal plane) at the laser intensity of 440 μW for 532 nm, while slightly larger intensity, 500 μW, was necessary for the 690-nm laser to attain the similar fluctuation. The weaker laser intensity at 532 nm than that at 690 nm is mainly attributed to the smaller focus spot. Actually, the wavelength dependence of scattering cross sections of the PMP leading to the difference of F_{sca} is quite small in this wavelength region on the basis of Mie calculation (See Figure S4 in S.I.).[24,25] In addition, wavelength dependence of F_{grad} is not significant in this wavelength region, because of the constant optical response of the PMP in visible wavelength region.

Before the discussion on the wavelength dependence of the trapping laser, we first show the Z-displacement as a function of original diameters of the trapped PMP at the trapping wavelength of 690 nm in Fig. 3a. Size distribution of the PMPs (7 ± 2 μm) affects the Z-displacements. At a UV laser intensity of 33 mW cm^{-2} (black filled triangles), the Z-displacements were not detectable for the PMPs larger than 8 μm in diameter. In contrast, the Z-displacements reached ca. 200 nm for the PMPs with diameters ranging from 4 to 6 μm. With an increase in the UV laser intensity, the Z-displacement increases and a maximum value of *ca.* 800 nm was observed (red open squares). This result indicates that the amount of the TC isomer in the PMP increased with increasing UV laser intensity, resulting in an increase in F_{abs} acting on the PMP. On the other hand, large-sized PMPs exhibited smaller Z-displacements even at the high UV laser intensity. That is, an increase in F_{grad} for larger PMPs under one irradiation condition results in a decrease in Z-displacement and the gravitational force ($F_{gravity}$) acting as a counter for F_{abs} for larger PMPs. That is, a weakening of F_{grad} results in larger Z-displacements at a constant F_{abs}.

Fig. 3b shows the Z-displacement as a function of original diameters of the trapped PMP at the trapping wavelength of 532 nm. At the UV laser intensity of 70 mW cm^{-2}, a mean Z-displacement was *ca.* 100 nm. As the UV laser intensity increases, the mean Z-displacement increases up to *ca.* 600 nm. In particular, the maximum Z-displacements for smaller PMPs at the high UV intensity were larger than 1 μm. Moreover, the Z-displacements for the PMPs larger than 8 μm in diameter were much greater than those observed for the trapping at 690 nm at the equivalent UV laser intensities. These differences in Z-displacement of the PMPs indicates that F_{abs} acting on the PMP is significantly wavelength dependent.

To more clearly visualize the trapping wavelength dependence, the mean Z-displacements at each wavelength are plotted as a function of the UV laser intensity in Fig. 3c. Although the Z-displacement linearly increases with UV laser intensity in both conditions with different color lasers, an increment in the Z-displacement under the 690-nm trapping is smaller than that by the 532-nm laser. The slope of the linear curves with the intercept of zero was 1.08 and 0.37 for 532 nm and 690 nm, respectively. That is, the slope for the 532-nm trapping was almost 3 times larger than that at 690 nm. This wavelength dependence reflects the absorption spectrum of the TC isomer of PQ. As shown in Fig. 1b, the ratio of the absorbance of the TC isomer in toluene at 532 nm and that at 690 nm was 19.1. On the other hand, the *Δextinction* spectrum of the TC isomer in the PMP was extended by 50 nm to longer wavelength region than that in toluene solution (See Figure S1 in S.I.). The ratio of *Δextinction* coefficients of the TC isomer at 532 and that 690 nm is 2.96 in the PMP, which is consistent with the trapping wavelength dependence observed in Fig. 3c.

To quantitatively verify the role of *Δextinction* coefficients at the trapping wavelength, we review the fundamental equation representing all optical forces acting on the PMP[7,8], F_{grad}, F_{sca}, and F_{abs}. First, as already mentioned in the previous section, F_{grad} was normalized by monitoring the positional fluctuations of the trapped PMP at each trapping wavelength. Second, in principle, scattering force is proportional to the scattering cross section (C_{sca} / m^2) of the PMP at the trapping wavelength, *i.e.* $F_{sca} \propto C_{sca}$. To compare C_{sca} at 532 and 690 nm, we calculated a scattering spectrum of a bare PMP in water on the basis of Mie theory.[24,25] As a result, we confirmed that the wavelength dependence of C_{sca} is much smaller than that of *Δextinction* coefficients in visible wavelength region (See Figure S4 in S.I.). Accordingly, one can safely conclude that small differences in F_{grad} and F_{sca} at each trapping wavelength do not result in the significant trapping wavelength dependence. Finally, absorption force is proportional to the *Δextinction* coefficients of

the TC isomer at the trapping wavelength, *i.e.* $F_{abs} \propto \Delta extinction$. Summarizing above discussion, we can conclude that the trapping wavelength dependence observed in Fig. 3c can be ascribed to F_{abs} arising from the TC isomer. This result directly indicates that radiation force acting on small objects is modulated by using photochromic reactions. Note that the real part of refractive index of the PMP changes due to photoisomerization. Because the real part corresponds to scattering force, the $\Delta extinction$ spectrum shown in Fig. S1b should be separated into absorption and scattering.[26,27] On the other hand, it has been reported that both thermophoresis[28] and fluid convection[29] can contribute to migration of small objects exposed to intense light fields. In the present case, an increase in temperature of the trapped PMP is expected to be less than a few Kelvin on the basis of heat conduction equations.[30–32] That is, the contribution of temperature-induced migration is safely excluded.

Dynamics of trapped microparticles: time constants of the displacement and their relation to photochromic reactions. In Fig. 4a, we show the time profile of the displacement of PMP under the laser trapping at 532 nm. The UV laser (278 mW cm^{-2}) was turned on at 2 s and irradiated the PMP for 2 s (until 4 s in the figure). The PMP started to move along the Z-axis after the turn-on of the UV irradiation and the Z-displacement of ca. 1 μm was attained around 3.7 s. We define the movement leaving from the original position before the UV irradiation as forward motion (F-motion). After the turn-off of the UV laser at 4 s, the PMP gradually returns to the original position before the UV irradiation. We define the displacement returning to the original position as the backward motion (B-motion). The time required for the half of the displacement of F- and B-motions is used as the time constant for the displacement in the following.

Fig. 4b shows the time constants of F- and B-motions of the PMP at the trapping wavelength of 690 nm. The time constants of the F-motion were ca. 0.4 s and not so strongly dependent on the UV laser power. In contrast, the mean time constant of the B-motion was ca. 0.8 s, which is two times greater than that of the F-motion. On the other hand, both time constants of F- and B-motions under the 532-nm trapping increase with increasing UV laser intensity as shown in Fig. 4c. This dependence on the UV laser intensity is attributable to much larger Z-displacements at high UV laser intensities.

In general, the dynamics of the movement of the present PMP is regulated by four factors, gravitational force, viscous drag, photoisomerization of CF to TC, and thermal back reaction of TC to CF. First, we consider dynamics on the photoisomerization of CF to TC. Because the ring-opening reaction takes place in the electronically excited state, the time constant of the reaction in molecular level[19] is in the time range $< 10^{-9}$-10^{-12} s. The growth of the TC isomer in PMP is, however, dependent on the intensity of UV light. The viscous drag[32] in water is diameter-dependent and affect the displacement of the PMP. In the case that both F- and B-motions are regulated mainly by the viscous drag, both time constants of F- and B- motions should be similar values. Moreover, under the the present experimental setup with the inverted optical microscope, the gravitational force could accelerate the B-motion.[23] The time constant of the B-motion is much slower than that of the F-motion. This result indicates that the viscous drag is not a main factor regulating the speed of the motions and suggests that the B-motion is regulated by the thermal back reaction of the TC- to CF isomers. Hence, we conclude that the spatiotemporal control of radiation force acting on the PMP is possible by using photochromic reactions of PQ.

Non-coaxial irradiation: 3D control of trapped microparticles. In previous sections, the UV laser and the trapping lasers were coaxially introduced. In this section, the configuration of irradiation was modified as shown in Fig. 5a. The UV laser was focused in such a manner that the optical axis is displaced 3.7 μm away from the optical axis of the trapping laser along X-axis. The spot diameter of the UV laser was 3.7 μm (in fwhm). In this configuration, the colorization reaction of PQ is partially induced on the PMP surface. Therefore, the trapped PMP is expected to be pushed not only to Z-direction, but also to the horizontal direction. In this experiment, the trapping laser intensity at 690 nm was set to 1 mW. An irradiation period of the UV laser was 7 s.

Fig. 5 b to –e shows a series of snapshots on the non-coaxial irradiation. In Fig. 5b, the PMP was trapped by the focused red laser at 0 s. Fig. 5c shows the transmission image of the PMP just after the start of the UV exposure at the excitation intensity of 15.4 W cm^{-2}. The PMP was partially colored, indicating an increase in the TC isomer. At the boundary region of the PMP and water (left hand side of the PMP), a weak emission signal was observed. This originates from photodegradation of PQ due to the intense UV irradiation. Fig. 5d shows the transmission image of the PMP after shutting off the UV exposure for 7 s. The center of the PMP moved along X-axis. This X-displacement could be attributed to the F_{abs} partially acting on left hand side of the PMP. At 25 s, the PMP came back to its original position by F_{grad} of the trapping laser (Fig. 5e). From a series of transmission images, trajectories of the weight center along X- and Y-axis were extracted as shown in Fig. 5f. Although no detectable change was observed for Y-displacement, the X-position of the PMP was observed at 3 s after the irradiation of the UV light. The X-displacement gradually increased with an increase in the time and reached the maximum value of 2 μm. After the UV laser was turned off at 10 s, the PMP gradually returned to the original position at ca. 17 s.

To verify the observed X-displacement was caused by F_{abs} of PQ, we performed a control experiment using bare PMPs under same irradiation condition. As a result, the bare PMP was slightly attracted to the focal spot of the UV laser; *i.e.* negative X-displacement. Therefore, the positive X-displacement observed in Fig. 5f can be ascribed to F_{abs} acting onto left hand side of the PMP.

In Fig. 5g, we plotted the temporal profile along the Z-axis. Interestingly, we could observe the Z-displacement increase by ca. 100 nm while the UV laser was turned on. This result indicates that the PMP was pushed not only to X-direction, but also to Z-direction and that 3D control of positions of the PMP is possible by using photochromic reactions of PQ.

So as to more quantitatively elucidate observed phenomena, numerical simulations of the optical field such as the trapping potential should be performed to estimate F_{abs} (*i.e.* a number of colored isomers in a microparticle). To calculate these fields and forces, simplified analytical solutions can be applied if the trapped particles are Rayleigh particles.[33,34] However, it is expected that the numerical simulation for the present system would be very complicated because the size of the trapped microparticle is much larger than the size of the laser spot. Therefore, full computation of the electric field including the trapping laser, the PMP, and water in a realistic geometry will be required. This is far beyond the scope at this moment, but we will perform it in future work.

Conclusions We employed photochromic reactions to modulate radiation force acting on the optically trapped PMP. For this purpose, pyranoquinazoline (PQ) derivatives were incorporated

into polymer microparticles with diameters of 7 μm. In the experiments, the colorization reaction of PQ in the trapped PMP was observed by irradiating the UV laser. It was demonstrated that the Z-displacement of the PMP was linearly proportional to the UV laser intensity, and was dominated by the *Δextinction* coefficients of PQ at the trapping wavelengths. Further, the analysis on dynamics of the PMP revealed that the B-motion of the PMP was affected by the thermal back reaction of PQ. In the experiment under non-coaxial irradiation, 3D control of the PMP was demonstrated by F_{abs} partially acting on the PMP. Thus, we have demonstrated the spatiotemporal control of radiation force by using organic photochromic compounds for the first time. We believe that this insight will introduce a new strategy into photo-control of nano-objects. Hereafter, we will report relationships between dynamics of the trapped microparticles and the time constants of thermal back reactions of photochromic compounds by using various kinds of pyranoquinazoline and naphthopyran derivatives.

Methods

Sample preparation The synthetic method of a pyranoquinazoline (PQ) derivative with a pyrenyl unit was already reported in our previous work in detail.[19] First, we prepared an acetonitrile (75-05-8, ∞pure, Wako) solution of PQ at a concentration of 0.25 mg mL^{-1}. Second, we added 10 mg of microparticles of polyacrylic ester resins (AFX-8, Sekisui Plastics) with diameters of 7.8 ± 2.4 μm into the solution. The solution was left for a few weeks for swelling of PQ into the polymer microparticles. After that, we put a few drops of the colloidal solution onto a glass coverslip (borosilicate glass, 24 × 32 × 0.17 mm, Matsunami) and dried it at atmospheric condition. Then

the polymer microparticles on the glass were submerged in ultrapure water (Direct-Q UV, Millipore), in a 40 μL chamber consisting of two coverslips and a 0.3 mm thick silicone rubber spacer. By applying a mechanical stimulus to the sample chamber, the microparticles on the coverslip were redispersed into water.

Optical setup We used an inverted optical microscope (IX-70, Olympus) for all the optical measurements. To acquire optical micrographs, a monochromatic CCD (Infinity 3-1 URM, Lumenera) was employed. We used three CW lasers at wavelengths of 355, 532, and 690 nm. For the lasers of 355 and 532 nm, 2nd and 3rd harmonic lights of a fundamental wavelength of a CW Nd:YAG (3-band CW laser, Oxide) laser were used. For the laser of 690 nm, we used a diode laser (DL690-050-S, CrystaLaser). For optical trapping, a microscope objective (UPlanFLN, 100×, NA = 1.30, Olympus) was used. For micro-spectroscopy of single polymer microparticles, a microscope objective (LUCPlanFLN, 60×, NA = 0.70, Olympus) and a fiber-coupled spectrometer (SD-2000, Ocean Optics) were used. The optical setup is shown in Figure S5 in S.I.

FIGURES.

Figure 1

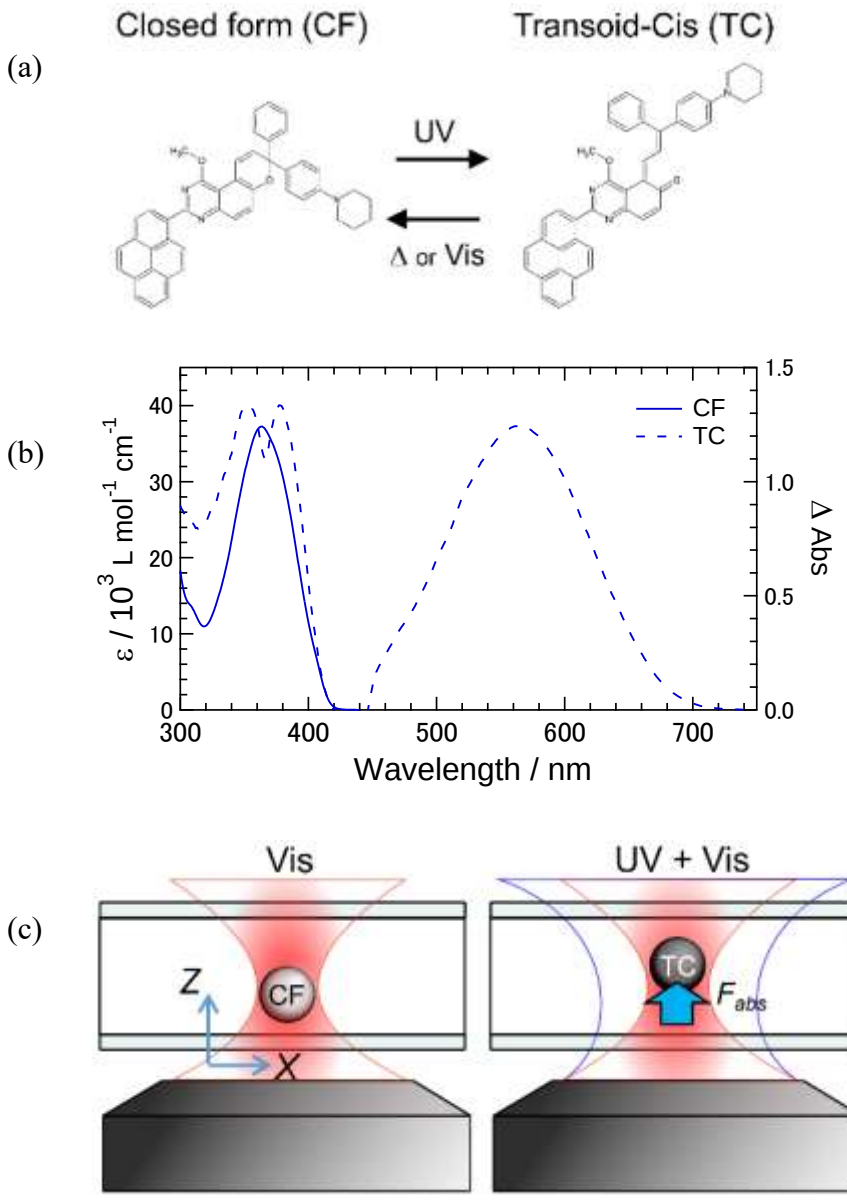

Figure 1. (a) Photochromic reactions of the 8H-pyranoquinazoline (PQ) derivative, 1-methoxy-8-phenyl-8-(4-(1-piperidinyl)phenyl)-3-(1-pyren-yl)-8H-pyrano[3,2-f]quinazoline. (b) UV-vis absorption spectra of PQ in CF isomer, and PQ in TC isomer under UV irradiation (365 nm, 440

mW cm^{-2}) in toluene at 298 K. (c) Schematic illustration of the switching of F_{abs} acting on a trapped microparticle by using the photochromic reactions of PQ.

Figure 2

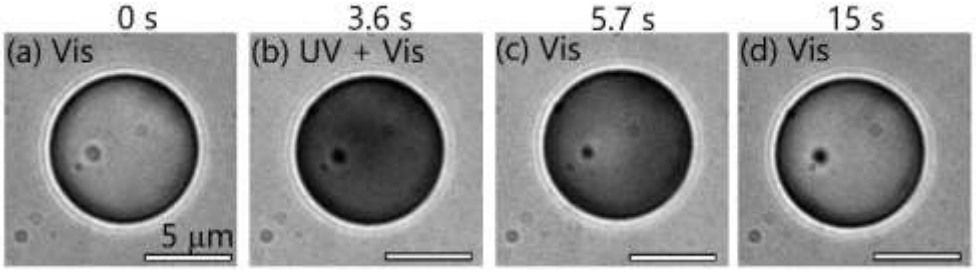

(e)

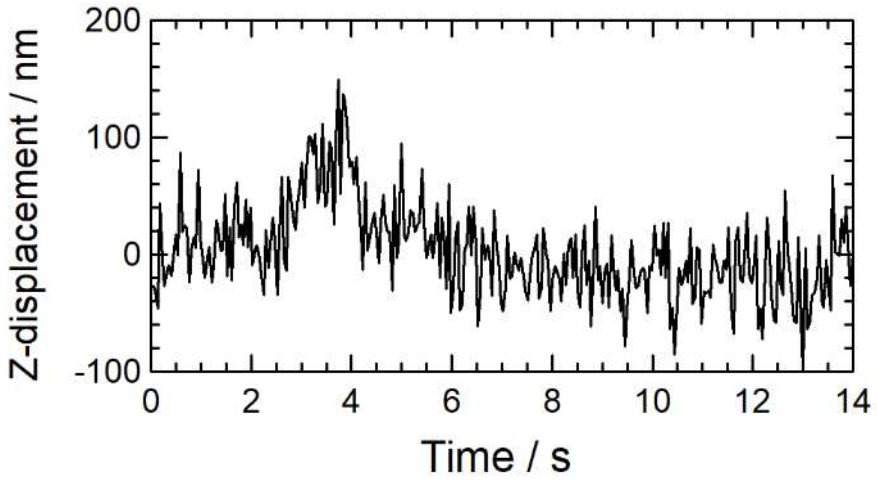

Figure 2. (a-d) Time course of transmission images of the polymer microparticle (PMP) trapped by the focused 690 nm CW laser at an intensity of 500 μW: the UV laser intensity was set to 400 mW cm^{-2}. The irradiation period of the UV laser was set to 2 s. (e) Time evolution of the Z-displacement of the PMP. The UV laser was introduced at 2 s, and it was turned off at 4 s.

Figure 3

(a)

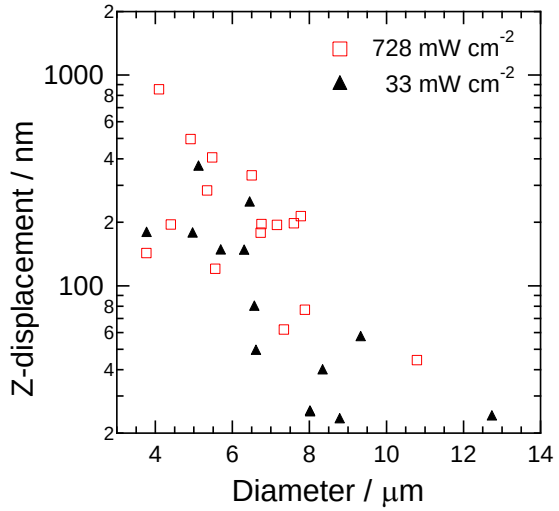
728 mW cm-2
33 mW cm-2
Z-displacement / nm
Diameter / μm

(b)

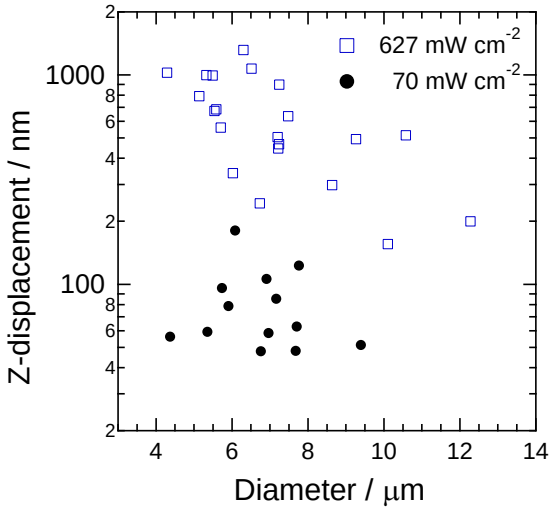
627 mW cm-2
70 mW cm-2
Z-displacement / nm
Diameter / μm

(c)

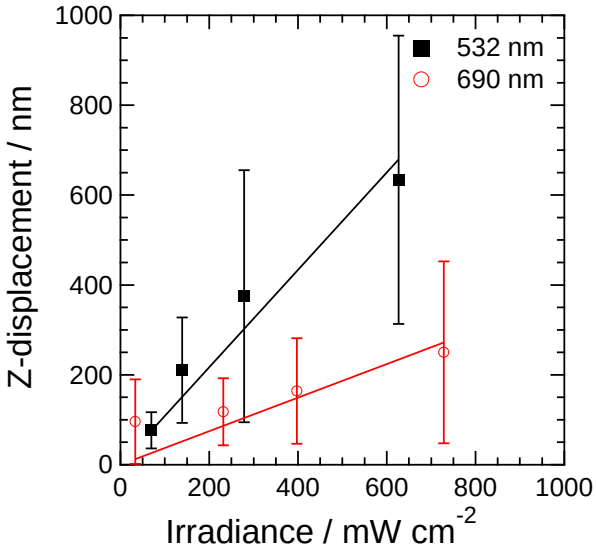
532 nm
690 nm
Z-displacement / nm
Irradiance / mW cm-2

Figure 3. Figure 3. (a) Z-displacements triggered by the UV irradiation as a function of the original diameter of the PMP at the trapping wavelength of 690 nm. (b) Z-displacements triggered by the UV irradiation as a function of the original diameter of the PMP at the trapping wavelength of 532 nm. (c) Mean Z-displacements as a function of the UV laser intensity.

Figure 4

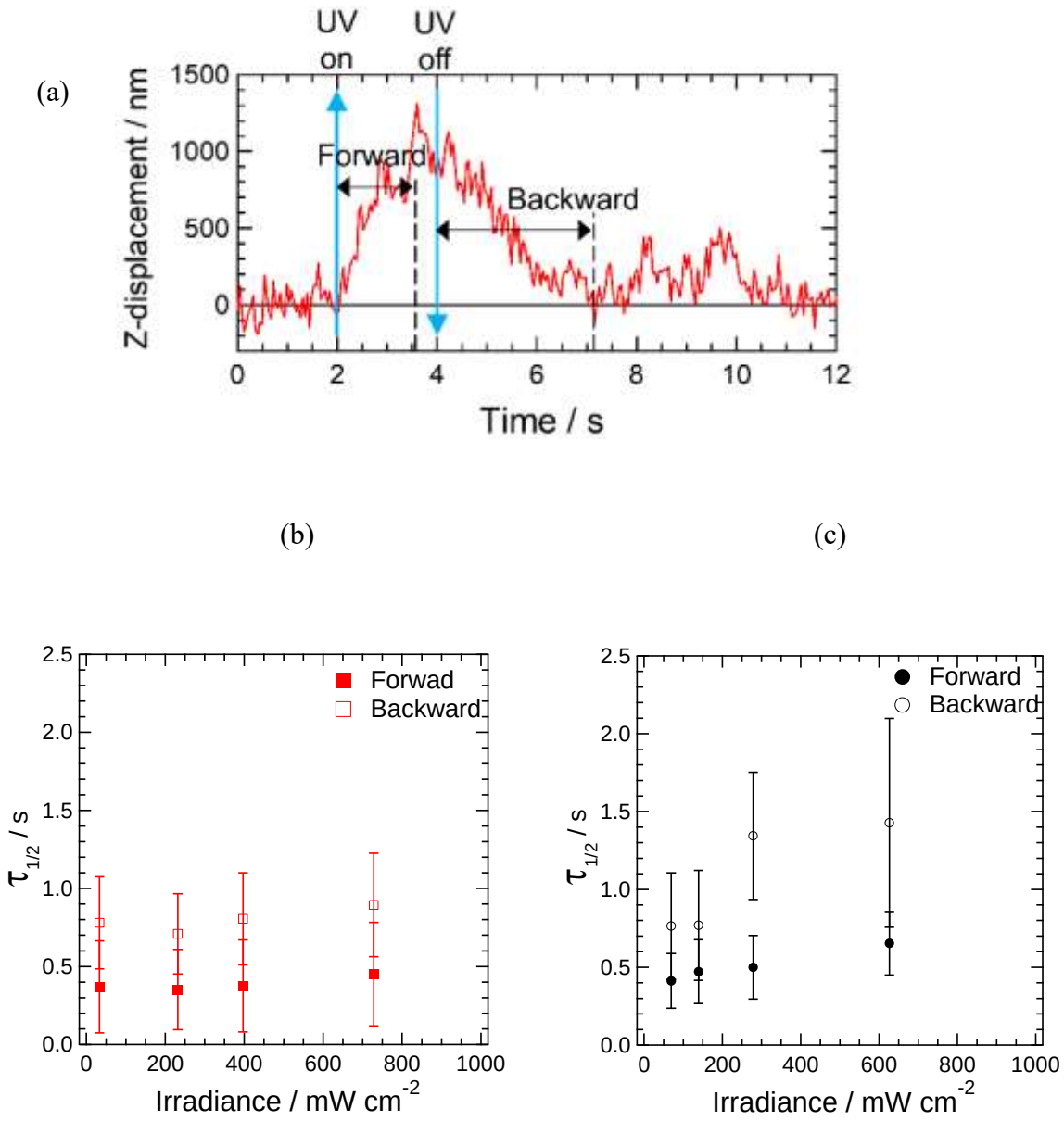

Figure 4. (a) Schematic representation of the definition of forward and backward motions of the PMP along Z-axis. The displayed time course of Z-displacement was measured at the UV laser intensity of 278 mW cm^{-2} and the trapping wavelength of 532 nm. (b) Time constants of the F-motion and the B-motion of the PMP as a function of the UV laser intensity at the trapping

wavelength of 690 nm. (c) Time constants of the F-motion and the B-motion of the PMP as a function of the UV laser intensity at the trapping wavelength of 532 nm.

Figure 5

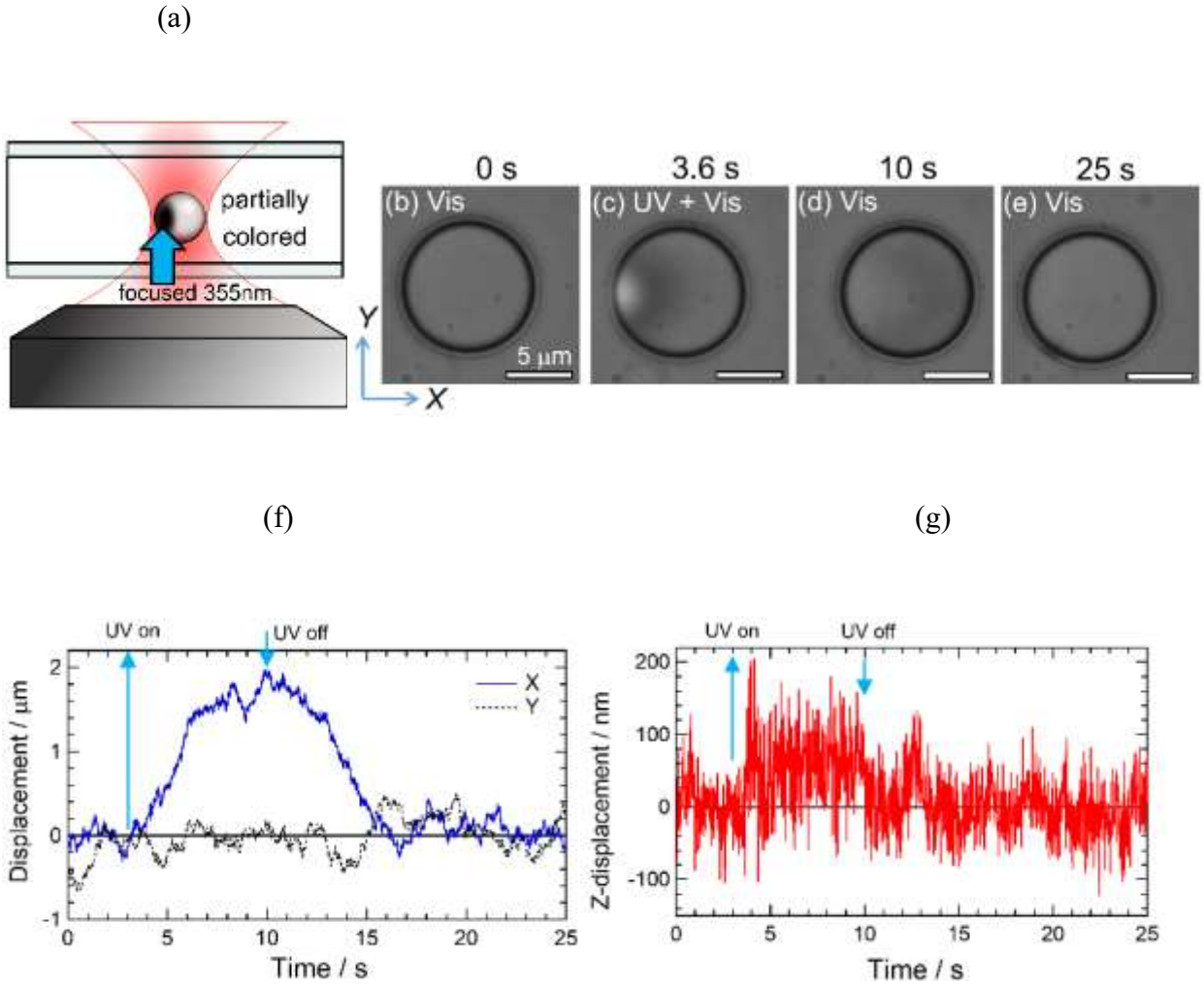

Figure 5. (a) Schematic illustration of the non-coaxial irradiation of the PMP. The focal spot of the UV laser is spatially displaced 3.7 μm away from the center of the 690 nm laser along X-axis. (b-e) Time course of optical transmission images of the PMP trapped by the focused 690 nm CW laser at an intensity of 1 mW: the UV laser intensity was set to 15.4 W cm^{-2}. The irradiation period of the UV laser was set to 7 s. (f) Time evolution of the displacements of the PMP along X- and Y- axis. The UV laser was introduced at 3 s, and it was turned off at 10 s. (g) Time evolution of the Z-displacement of the PMP corresponding to Fig. 5f

ASSOCIATED CONTENT

AUTHOR INFORMATION

Corresponding Author

* sito@chem.es.osaka-u.ac.jp. * miyasaka@chem.es.osaka-u.ac.jp.

Division of Frontier Materials Science and Center for Promotion of Advanced Interdisciplinary Research, Graduate School of Engineering Science, Osaka University, Toyonaka, Osaka 560-8531, Japan.

Author Contributions

K.S. and A.M.M. performed experiments and analyses of optical trapping. Y.I., K.M., and J.A. prepared and evaluated the samples. S.I. and H.M. designed the concept of the present work. K.S., S.I., and H.M. prepared the manuscript with contributions from all authors. All authors have given approval to the final version of the manuscript.

Notes

The authors declare no competing financial interest.

ACKNOWLEDGMENT

This study was financially supported by JSPS KAKENHI Grant Numbers JP26107002, JP26107010, JP16H06505 and JP16H03827. We sincerely thank Prof. Yoichi Kobayashi of Ritsumeikan University for stimulating discussion

Supporting Information. Scattering micro-spectroscopy of the PMP incorporating PQ, a control experiment for optical trapping using a bare PMP and, a control experiment for the detection of Z-displacement of the PMP, a calculated scattering spectrum of a PMP in water, and schematic illustration of optical setup. This material is available free of charge via the Internet at http://pubs.acs.org.

REFERENCES

(1) Grier, D. G. A Revolution in Optical Manipulation. *Nature* **2003**, *424*, 810–816.

(2) Yu, Y.; Nakano, M.; Ikeda, T. Directed Bending of a Polymer Film by Light. *Nature* **2003**, *425*, 145–145.

(3) Lendlein, A.; Jiang, H.; Jünger, O.; Langer, R. Light-Induced Shape-Memory Polymers. *Nature* **2005**, *434*, 879–882.

(4) Kobatake, S.; Takami, S.; Muto, H.; Ishikawa, T.; Irie, M. Rapid and Reversible Shape Changes of Molecular Crystals on Photoirradiation. *Nature* **2007**, *446*, 778–781.

(5) Irie, M.; Fukaminato, T.; Matsuda, K.; Kobatake, S. Photochromism of Diarylethene Molecules and Crystals: Memories, Switches, and Actuators. *Chem. Rev.* **2014**, *114*, 12174–12277.

(6) Ashkin, A. Acceleration and Trapping of Particles by Radiation Pressure. *Phys. Rev. Lett.* **1970**, *24*, 156–159.

(7) Ashkin, A.; Dziedzic, J. M.; Bjorkholm, J. E.; Chu, S. Observation of a Single-Beam Gradient Force Optical Trap for Dielectric Particles. *Opt. Lett.* **1986**, *11*, 288–290.

(8) Neuman, K. C.; Block, S. M. Optical Trapping. *Rev. Sci. Instrum.* **2004**, *75*, 2787–2809.

(9) Ashkin, A. History of Optical Trapping and Manipulation of Small-Neutral Particle, Atoms, and Molecules. *IEEE J. Sel. Top. Quantum Electron.* **2000**, *6*, 841–856.

(10) Curtis, J. E.; Grier, D. G. Structure of Optical Vortices. *Phys. Rev. Lett.* **2003**, *90*, 133901.

(11) Toyoda, K.; Miyamoto, K.; Aoki, N.; Morita, R.; Omatsu, T. Using Optical Vortex to Control the Chirality of Twisted Metal Nanostructures. *Nano Lett.* **2012**, *12*, 3645–3649.

(12) Maurer, C.; Jesacher, A.; Bernet, S.; Ritsch-Marte, M. What Spatial Light Modulators Can Do for Optical Microscopy. *Laser Photon. Rev.* **2011**, *5*, 81–101.

(13) Juan, M. L.; Righini, M.; Quidant, R. Plasmon Nano-Optical Tweezers. *Nat. Photonics* **2011**, *5*, 349–356.

(14) Shoji, T.; Tsuboi, Y. Plasmonic Optical Tweezers toward Molecular Manipulation: Tailoring Plasmonic Nanostructure, Light Source, and Resonant Trapping. *J. Phys. Chem. Lett.* **2014**, *5*, 2957–2967.

(15) Kudo, T.; Ishihara, H. Proposed Nonlinear Resonance Laser Technique for Manipulating Nanoparticles. *Phys. Rev. Lett.* **2012**, *109*, 87402.

(16) Inaba, K.; Imaizumi, K.; Katayama, K.; Ichimiya, M.; Ashida, M.; Iida, T.; Ishihara, H.; Itoh, T. Optical Manipulation of CuCl Nanoparticles under an Excitonic Resonance Condition in Superfluid Helium. *Phys. Status Solidi Basic Res.* **2006**, *243*, 3829–3833.

(17) Tamai, N.; Miyasaka, H. Ultrafast Dynamics of Photochromic Systems. *Chem. Rev.* **2000**, *100*, 1875–1890.

(18) Kobayashi, Y.; Mutoh, K.; Abe, J. Fast Photochromic Molecules toward Realization of Photosynergetic Effects. *J. Phys. Chem. Lett.* **2016**, *7*, 3666–3675.

(19) Inagaki, Y.; Kobayashi, Y.; Mutoh, K.; Abe, J. A Simple and Versatile Strategy for Rapid Color Fading and Intense Coloration of Photochromic Naphthopyran Families. *J. Am. Chem. Soc.* **2017**, *139*, 13429–13441.

(20) Mutoh, K.; Kobayashi, Y.; Abe, J. Efficient Coloration and Decoloration Reactions of Fast Photochromic 3H-Naphthopyrans in PMMA-B-PBA Block Copolymer. *Dye. Pigment.* **2017**, *137*, 307–311.

(21) Speidel, M.; Jonáš, A.; Florin, E.-L. Three-Dimensional Tracking of Fluorescent Nanoparticles with Subnanometer Precision by Use of off-Focus Imaging. *Opt. Lett.* **2003**, *28*, 69–71.

(22) Lee, S.-H.; Roichman, Y.; Yi, G.-R.; Kim, S.-H.; Yang, S.-M.; Blaaderen, A. van; Oostrum, P. van; Grier, D. G. Characterizing and Tracking Single Colloidal Particles with Video Holographic Microscopy. *Opt. Express* **2007**, *15*, 18275.

(23) Nedev, S.; Carretero-Palacios, S.; Kühler, P.; Lohmüller, T.; Urban, A. S.; Anderson, L. J. E.; Feldmann, J. An Optically Controlled Microscale Elevator Using Plasmonic Janus Particles. *ACS Photonics* **2015**, *2*, 491–496.

(24) Garcia, M. A. Surface Plasmons in Metallic Nanoparticles: Fundamentals and Applications. *J. Phys. D. Appl. Phys.* **2011**, *44*, 283001.

(25) Setoura, K.; Werner, D.; Hashimoto, S. Optical Scattering Spectral Thermometry and Refractometry of a Single Gold Nanoparticle under CW Laser Excitation. *J. Phys. Chem. C* **2012**, *116*, 15458–15466.

(26) Juodkazis, S.; Mukai, N.; Wakaki, R.; Yamaguchi, A.; Matsuo, S.; Misawa, H. Reversible Phase Transitions in Polymer Gels Induced by Radiation Forces. *Nature* **2000**, *408* (6809), 178–181.

(27) Ito, S.; Mitsuishi, M.; Setoura, K.; Tamura, M.; Iida, T.; Morimoto, M.; Irie, M.; Miyasaka, H. Mesoscopic Motion of Optically Trapped Particle Synchronized with Photochromic Reactions of Diarylethene Derivatives. *J. Phys. Chem. Lett.* **2018**, *9*, 2659–2664.

(28) Jiang, H. R.; Wada, H.; Yoshinaga, N.; Sano, M. Manipulation of Colloids by a Nonequilibrium Depletion Force in a Temperature Gradient. *Phys. Rev. Lett.* **2009**, *102*, 208301.

(29) Setoura, K.; Ito, S.; Miyasaka, H. Stationary Bubble Formation and Marangoni Convection Induced by CW Laser Heating of a Single Gold Nanoparticle. *Nanoscale* **2017**, *9*, 719–730.

(30) Govorov, A. O.; Richardson, H. H. Generating Heat with Metal Nanoparticles. *Nano Today* **2007**, *2*, 30–38.

(31) Baffou, G.; Quidant, R. Thermo-Plasmonics: Using Metallic Nanostructures as Nano-Sources of Heat. *Laser Photon. Rev.* **2013**, *7*, 171–187.

(32) Ito, S.; Sugiyama, T.; Toitani, N.; Katayama, G.; Miyasaka, H. Application of Fluorescence Correlation Spectroscopy to the Measurement of Local Temperature in Solutions under Optical Trapping Condition. *J. Phys. Chem. B* **2007**, *111*, 2365.

(33) Svoboda, K.; Block, S. M. Optical Trapping of Metallic Rayleigh Particles. *Opt. Lett.* **1994**, *19*, 930–932.

(34) Bendix, P. M.; Jauffred, L.; Norregaard, K.; Oddershede, L. B. Optical Trapping of Nanoparticles and Quantum Dots. *IEEE J. Sel. Top. Quantum Electron.* **2014**, *20*, 4800112.

Table of Contents Graphic